Check for updates

Highly efficient and recyclable chiral phosphine-functionalized polyether ionic liquids for asymmetric hydrogenation of β-keto esters†

Fan Wang, [ab] Shuai Zhang,[b] Congxia Xie [a] and Xin Jin [*b]

Herein, based on the concept of integration of phosphine ligands and ionic liquids (ILs), a class of chiral phosphine-functionalized polyether ionic liquids (CPF-PILs) were synthesized by ion-exchange reaction between polyether imidazolium ILs and a phenyl-sulfonated (S)-(−)-2,2′-bis(diphenylphosphino)-1,1′-binaphthyl (BINAP) chiral diphosphine ligand, and employed in the Ru-catalyzed homogeneous asymmetric hydrogenation of β-keto esters. The resulting CPF-PILs combined the dual functions of the chiral phosphine ligand and ILs, allowing efficient recovery and recycling of the chiral catalysts using only a catalytic amount of CPF-PILs. The effects of various factors, including the chiral catalyst structure, solvent properties, reaction temperature, hydrogen pressure, and hydrobromic acid dosage, on catalytic performance were thoroughly investigated, as well as the cycling stability and universality of the chiral catalysts were examined. The findings of the present study demonstrated that, under optimal reaction conditions, the model substrate methyl acetoacetate underwent quantitative conversion to methyl β-hydroxybutyrate with a 97% enantiomeric excess (ee). The chiral catalyst used in this process can be recycled up to 12 times and showed good applicability to structurally various β-keto esters. The present study presents a novel approach for using ILs in asymmetric hydrogenation reactions in an environmentally friendly manner.

1   Introduction

Since the 1960s, significant progress has been made in developing asymmetric catalytic hydrogenation.[1,2] This type of reaction can transform affordable and readily available prochiral compounds into optically pure substances with promising applications in pharmaceuticals, fragrances, and agrochemicals.[3] Nevertheless, separating, recovering, and recycling expensive chiral noble metal catalysts remains a great challenge for the industrialization of asymmetric catalytic hydrogenation.[4]

Because of their low vapor pressure, non-flammability, good chemical and thermal stability, excellent solubility for substrates and chiral catalysts, and structural designability,[5,6] ionic liquids (ILs) have been widely used as green solvents and catalyst carriers in various asymmetric catalytic reactions and organic synthesis.[7–9] Despite the significant progress in applying ILs, certain limitations remain. Using large amounts of high-viscosity ILs has decreased mass transfer efficiency,

impacting catalytic activity and selectivity.[10,11] This deviation from green chemistry principles undermines the desired outcomes and introduces additional costs. Consequently, reducing the dosage of ILs while ensuring efficient catalysis is a formidable challenge that must be overcome as ILs progress toward practical implementation.

In previous studies, we have developed a series of phosphine-functionalized polyether ionic liquids (PF-PILs) based on the concept of integrated phosphine ligands and ILs[12,13] and used them in the hydroformylation of olefins[10,14] and asymmetric hydrogenation of β-keto esters.[15] Because these PF-PILs have the unique ability to act as both a phosphine ligand and an ionic liquid (IL), only catalytic amounts of PF-PILs were required for catalytic reactions, enabling efficient catalyst separation and recycling without the need for excessive amounts of additional carrier ILs, thereby significantly reducing the dosage of ILs. The successful application of PF-PILs encouraged us to further explore the applicability of this concept to other sulfonated phosphine ligands.

In this paper, we synthesized two novel chiral phosphine-functionalized polyether ionic liquids (CPF-PILs) (3, Fig. 1) by ion-exchange reactions of phenyl-sulfonated BINAP chiral diphosphine ligand (1, Fig. 1) and polyether imidazolium ILs (2, Fig. 1) and used them in the Ru-catalyzed asymmetric hydrogenation of β-keto esters. The Ru-3 catalyst has comparable enantioselectivity, higher catalytic activity than the parent Ru-1

[a] College of Chemistry and Molecular Engineering, Qingdao University of Science and Technology, 53 Zhengzhou Road, Qingdao 266042, China

[b] College of Chemical Engineering, Qingdao University of Science and Technology, 53 Zhengzhou Road, Qingdao 266042, China. E-mail: jinx1971@163.com

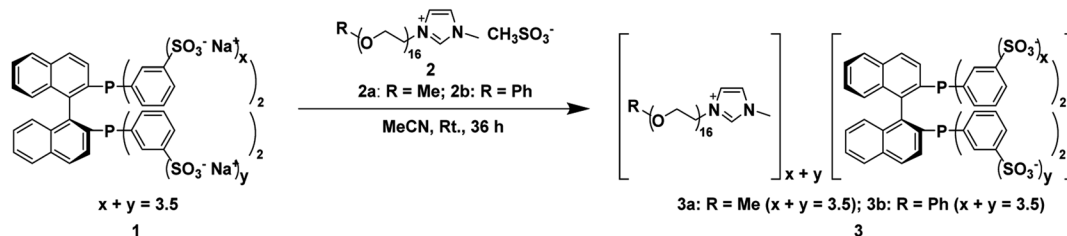† Electronic supplementary information (ESI) available. See DOI: https://doi.org/10.1039/d3ra05087d

Fig. 1 Synthesis of CPF-PILs based on phenyl-sulfonated BINAP and polyether imidazolium ILs.

catalyst, and good tolerance to solvents of different polarities and substrate generalizability. Simultaneously, Ru-**3** can be recycled 12 times and has high long-term stability.

2 Experimental

2.1 General information

BINAP (purity 99%) was purchased from Xinxiang Runyu Material Co., Ltd. in China. Bis (2-methylallyl)(1,5-cyclooctadiene) ruthenium(II) (Ru[[(2-methylallyl)$_2$(COD)], purity 97%), hydrobromic acid (48%) and β-keto ester were supplied by Shanghai Aladdin Chemical Reagent Co., Ltd. H$_2$ with a purity of 99.999% was purchased from Qingdao Deyi Gas Co., Ltd. The phenyl-sulfonated BINAP **1** was synthesized using a method described in the literature.[16] The polyether ILs **2** were synthesized according to the literature.[17] All experiments were performed under an argon atmosphere using standard Schlenk techniques. Solvents and reagents were dried and deoxygenated before use by a solvent purification system.[18]

^{1}H, ^{13}C, and ^{31}P NMR data were collected using a Bruker AVANCE 500 MHz or an AVANCE III 600 instrument. The HRMS spectra were recorded using a Thermo Fisher Scientific LTQ Orbitrap XL mass spectrometry. An IRIS Intrepid II XSP apparatus collected ICP-AES data to measure Ru and P leaching. Thermogravimetric analysis (TG) was determined from 30 °C to 700 °C under N$_2$ flow using a PerkinElmer STA 8000 Simultaneous Thermal Analyzer and a ramp rate of 10 °C min^{-1}. The asymmetric hydrogenation reaction was conducted in a 60 mL stainless high-pressure autoclave (316 L). The yield and ee values of the product were determined using a gas chromatography (GC) SP-2100A GC system equipped with a Supelco γ-dex 225 chiral capillary column (30 m × 0.25 mm × 0.25 μm). The chromatographic conditions were as follows: detector temperature 250 °C, injector temperature 220 °C, high purity N$_2$ as the carrier gas, flow rate 40 mL min^{-1}, splitting ratio 40 : 1, column temperature 70 °C, and maintained for 60 min. At 30% conversion, the turnover frequency was calculated by recording the hydrogen pressure drop, thus denoted as TOF$_{30}$.

2.2 Preparation of 3 and their characterizations

The sulfonated BINAP chiral diphosphine ligand **1** (0.7 g, 0.71 mmol) and polyether IL **2a** (2 g, 2.23 mmol) were added to a 100 mL Schlenk reaction flask with 20 mL of acetonitrile in an argon atmosphere. The reaction mixture was flash-frozen in liquid nitrogen and replaced with argon gas thrice. The reaction

was stirred at room temperature for 36 h. After the reaction, the mixture was filtered, and the solvent was removed from the filtrate under reduced pressure to give a pale yellow viscous liquid **3a** (2.20 g, 0.59 mmol) in 83% yield. The same synthetic method obtained **3b** in 91% yield.

2.2.1 Characterization. 3a: ^{1}H NMR (500 MHz, CDCl$_3$): δ = 9.64 (s, 3.5H, CH$_{imid}$–H), 9.04 (d, 2H, J = 10 Hz, CH$_{Naphthyl}$–H), 8.07 (t, 2H, J = 5 Hz, CH$_{Naphthyl}$–H), 7.52 (t, 3.5H, J = 1 Hz Ch$_{imdi}$–H), 7.46 (dd, 2H, J$_1$ = 7.5 Hz, J$_2$ = 2 Hz, CH$_{Naphthyl}$–H), 7.22 (s, 3.5H, CH$_{imid}$–H), 7.13–7.02 (m, 20H, CH$_{Naphthyl}$–H & CH$_{ph}$–H), 6.82 (d, 2H, J = 2 Hz, CH$_{Naphthyl}$–H), 4.38 (t, 7H, J = 4.5 Hz, N–CH$_2$), 3.84 (s, 10.5H, N–CH$_3$), 3.77 (t, 7H, J = 4 Hz, CH$_3$–O–CH$_2$), 3.64–3.52 (m, 204H, OCH$_2$CH$_2$), 3.36 (s, 10H, PEG-OCH$_3$) ppm; ^{13}C NMR (126 MHz, CD$_3$OD): δ = 146.78 (d), 142.75 (s), 139.58 (s), 139.20 (s), 138.18 (d), 135.98(t), 134.51 (t), 132.69 (s), 131.85 (s), 130.42 (s), 129.91 (d), 129.61 (s), 128.52 (s), 127.78 (s), 125.90 (s), 125.13 (s), 124.73 (s), 73.48–71.85 (m), 70.26 (s), 59.62 (s), 51.32 (s), 37.12 (s) ppm; ^{31}P NMR (202 MHz, D$_2$O): δ = −15.46 ppm; HRMS (ESI positive): m/z calcd for [C$_{37}$H$_{73}$O$_{16}$N$_2$]$^+$ 801.4955, found 801.4956; HRMS (ESI negative): m/z calcd for [C$_{44}$H$_{29}$O$_9$S$_3$P$_2$]$^{3-}$ 286.3488 (z = 3), found 286.3489; m/z calcd for [C$_{44}$H$_{28}$O$_{12}$S$_4$P$_2$]$^{4-}$ 234.4990 (z = 4), found 234.4991; **3b:** ^{1}H NMR (500 MHz, DMSO-d$_6$): δ = 9.04 (s, 3.5H, CH$_{imid}$–H), 8.89 (d, 2H, J = 10 Hz, CH$_{Naphthyl}$–H), 7.84 (d, 2H, J = 5 Hz, CH$_{Naphthyl}$–H), 7.72 (s, 3.5H, CH$_{imid}$–H), 7.69 (s, 3.5H, CH$_{imid}$–H), 7.28–7.21 (m, 21H, CH$_{ph}$–H & CH$_{Naphthyl}$–H), 7.02–6.90 (m, 19.5H, PEG-OC$_6$H$_5$ & CH$_{Naphthyl}$–H), 6.76 (d, 2H, J = 10 Hz, CH$_{Naphthyl}$–H), 4.34 (t, 7H, J = 5 Hz, N–CH$_2$), 4.07 (t, 7H, J = 5 Hz, N–CH$_2$–CH$_2$), 3.86 (s, 10.5H, N–CH$_3$), 3.77–3.50 (m, 213H, OCH$_2$CH$_2$) ppm; ^{13}C NMR (151 MHz, DMSO-d$_6$): δ = 158.43 (s), 144.12 (s), 137.18 (s), 136.81 (s), 134.18 (s), 134.137 (s), 133.15 (t), 132.35 (t), 130.02 (s), 129.45 (s), 129.11 (s), 128.51 (s), 128.40–128.22 (m), 127.91 (s), 127.72 (s), 125.12 (s), 124.56 (s), 123.34 (s), 122.67 (s), 120.52 (s), 114.39 (s), 69.91–69.51 (m), 68.94 (s), 68.10 (s), 66.94 (s), 48.74 (s), 35.70 (s) ppm; ^{31}P NMR (202 MHz, CDCl$_3$): δ = −16.01 ppm; HRMS (ESI positive): m/z calcd for [C$_{42}$H$_{75}$O$_{16}$N$_2$]$^+$ 863.5111, found 863.5117; HRMS (ESI negative): m/z calcd for [C$_{44}$H$_{29}$O$_9$S$_3$P$_2$]$^{3-}$ 286.3488 (z = 3), found 286.3481; m/z calcd for [C$_{44}$H$_{28}$O$_{12}$S$_4$P$_2$]$^{4-}$ 234.4990 (z = 4), found 234.4993.

2.3 Preparation of chiral catalyst [(3)RuBr$_2$]

The chiral catalyst [(**3**)RuBr$_2$] was prepared using the method described in the literature.[19] Under an argon atmosphere, Ru[(2-methylallyl)$_2$(COD)] (1.0 mg, 0.00313 mmol) and **3a** (14 mg, 0.00375 mmol) were added to a 10 mL Schlenk tube, then 5.5 μL

methanol solution of HBr (1.91 M, 0.0105 mmol), 0.5 mL of acetone, and 1 mL of methanol were added sequentially and stirred at room temperature for 30 min. The brownish catalyst [(**3a**)RuBr$_2$] was obtained by evaporating the solvent under reduced pressure. Similarly, the chiral catalyst [(**3b**)RuBr$_2$] was prepared.

2.4 Ru-catalyzed asymmetric hydrogenation of β-keto esters and the general process of chiral catalyst cycling

A typical procedure was as follows: under an argon atmosphere, 0.34 mL (3.13 mmol) methyl acetoacetate and 2 mL methanol were sequentially added to the freshly prepared chiral catalyst [(**3a**)RuBr$_2$] (0.00313 mmol), mixed well, and transferred to a 60 mL autoclave, where the argon was replaced thrice. The temperature was then raised to the preset level, hydrogen gas at the specified pressure was introduced, and the reaction was magnetically stirred at 400 rpm for a predetermined reaction time. The reaction mixture was cooled with ice water to release hydrogen gas and then transferred to a 10 mL Schlenk tube under an argon atmosphere. Afterwards, methanol was removed using reduced pressure. The product was extracted using *n*-hexane (2 × 4 mL) and left in ice water. The upper *n*-hexane phase was separated by decantation, and GC analysis was performed to determine the yield and ee value of the product β-hydroxy ester. The lower catalyst phase solidifies and adheres to the vessel wall before being replenished with fresh methanol and substrate for the next catalytic cycle.
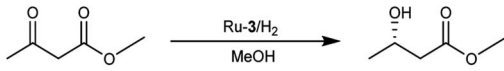
3 Results and discussion

3.1 Effect of structure of CPF-PILs on Ru-catalyzed asymmetric hydrogenation of methyl acetoacetate (MAA)

First, according to the literature,[16] the phenyl-sulfonated BINAP chiral diphosphine ligand **1** was synthesized by fuming sulfuric acid sulfonation. The average number of sulfonate groups on the four phenyl groups of **1** was 3.5 using ^{1}H NMR spectroscopy analysis. Then, we performed ion-exchange reactions of methyl- and phenyl-capped polyether imidazolium ILs **2a** and **2b** with **1** in acetonitrile at room temperature for 36 h, respectively, to obtain CPF-PILs **3a** and **3b** with 83% and 91% yield, respectively.

Ru-catalyzed homogeneous asymmetric hydrogenation of MAA was used as a model reaction to investigate the catalytic performance of CPF-PILs **3a** and **3b** with Ru-**1** as the reference catalyst. Table 1 indicated that in a homogeneous catalytic system with methanol as a solvent, both Ru-**3a** and Ru-**3b** quantitatively converted MAA to the target product methyl β-hydroxybutyrate (MHB) within 3 h, yielding TOF$_{30}$ values of 800 h^{-1} and 783 h^{-1}, respectively (entries 1 and 2, Table 1), which exhibited essentially comparable catalytic activities. In contrast, Ru-**1** produced MHB in quantitative yield in 20 h with a TOF$_{30}$ value of only 271 h^{-1} (entry 3, Table 1). Ru-**3a** and Ru-**3b** had the same enantioselectivity as Ru-**1**, with ee values of 97%, indicating that the introduction of the polyether imidazolium cation did not affect the enantioselectivity. Moreover, the activity-enhancing effect of catalysts Ru-**3a** and Ru-**3b** could be

Table 1 Effect of structures of CPF-PILs on Ru-**3**-catalyzed asymmetric hydrogenation of MAA^a

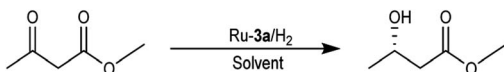| Entry	Catalyst	t/h	Yield^b/%	ee (S)^b/%	TOF$_{30}$/h^{-1}
1	Ru-**3a**	3	>99	97	800
2	Ru-**3b**	3	>99	97	783
3	Ru-**1**	20	>99	97	271

^{a} Reaction conditions: Ru[(2-methylallyl)$_2$(COD)]: 1 mg, catalyst loading 0.1 mol%, n(Ru):n(**3**):n(HBr):n(MAA) = 1:1.2:3.4:1000, 2 mL MeOH as solvent, P(H$_2$) = 4.6 MPa, T = 60 °C. ^{b} Analyzed by GC on a Supelco γ-dex 225 (30 m × 0.25 mm × 0.25 μm) chiral capillary column.

attributed to the fact that the steric hindrance created by the polyether chains effectively blocks the conversion of the monomeric catalytically active species [(**3**)RuBr$_2$] to the inactive dimer [(**3**)RuBr$_2$]$_2$, thereby increasing the concentration of the monomer species in the system, and enhancing the catalytic activity.[15] The primary subject of our subsequent investigation was the diphosphine ligand **3a**.

3.2 Effects of solvent on Ru-3a-catalyzed asymmetric hydrogenation of MAA

Numerous studies have demonstrated that solvent effects are critical in asymmetric hydrogenation reactions.[20,21] The solvent effects of several aprotic organic solvents with different polarities in the Ru-**3a**-catalyzed asymmetric hydrogenation of MAA were investigated in Table 2, with methanol as a reference. The Kamlet–Taft solvent polarity parameter, π*, was used to characterize the polarity of solvents.[22] By comparing the results, Ru-**3a** has the most outstanding catalytic efficiency in the proton solvent methanol, achieving 99% MHB yield and 97% ee value (entry 1, Table 2). This could be attributed to the fact that

Table 2 Solvent effect in Ru-**3a**-catalyzed asymmetric hydrogenation of MAA^a

Entry	Solvent	π*	Yield^b/%	ee (S)^b/%
1	MeOH^c	0.60	99	97
2	CH$_2$Cl$_2$	0.73	81	92
3	MeCN	0.66	59	90
4	THF	0.55	62	82
5	1,4-Dioxane	0.49	76	84
6	Toluene	0.49	64	86
7	EtOAc	0.45	34	31

^{a} Reaction conditions: Ru[(2-methylallyl)$_2$(COD)]: 1 mg, catalyst loading 0.1 mol%, n(Ru):n(**3a**):n(HBr):n(MAA) = 1:1.2:3.4:1000, 2 mL solvent, P(H$_2$) = 4.6 MPa, T = 60 °C, t = 20 h. ^{b} Analyzed by GC on a Supelco γ-dex 225 (30 m × 0.25 mm × 0.25 μm) chiral capillary column. ^{c} t = 3 h.

methanol has not only a high π^* value but also a strong hydrogen-bonding acidity, and these properties allow methanol to act as a proton source to facilitate the release of hydrogenation products from the catalytic active center during the catalytic cycle, while the hydrogen-bonding basicity of methanol is conducive to methanol acting as a temporary ligand to promote the catalytic reaction.[23] In contrast, the impact of solvent effects on the catalytic performance of Ru-**3a** in aprotic solvents was found to be significant, resulting in a significant reduction in both catalytic activity and enantioselectivity, leading to low to moderate yields of MHB. Our study revealed that the solvent polarity parameter π^* played an important role in determining the catalytic activity and ee value. As the π^* values of aprotic solvents decreased, the yields of MHB varied between 81% and 34% (entries 2–7, Table 2). In terms of enantioselectivity, as the π^* values decreased in the order of CH_2Cl_2 > MeCN > THF > 1,4-dioxane = toluene > EtOAc, the ee values presented an overall decreasing trend. It can be seen that increasing the polarity of aprotic solvent is helpful to improve the catalytic performance.

3.3 Effects of reaction parameters on Ru-3a-catalyzed asymmetric hydrogenation of MAA

The impact of reaction temperature on the Ru-**3a**-catalyzed asymmetric hydrogenation of MAA was investigated in Fig. 2A. The yields of MHB increased significantly from 32% to 99% as the temperature increased from 40 °C to 60 °C, and then remained essentially constant as the temperature increased further. However, the TOF_{30} value increased by *a* factor of 2–4 per 10 °C increase from 40 °C to 70 °C, consistent with general catalytic reaction kinetics principles. The enantioselectivity rose with increasing temperature, reaching a peak ee value of 97% at 60 °C before gradually declining. This phenomenon can be attributed to a decrease in the energy barrier disparity between the energetically dominant and the energetically inferior diastereomeric transition states within the catalytic reaction as a result of temperature elevation,[24] which led to a decrease in the enantioselectivity of the S-configuration. Therefore, the optimal reaction temperature for catalyst Ru-**3a** is 60 °C.

Fig. 2B depicted the effect of H_2 pressure on the Ru-**3a**-catalyzed homogeneous asymmetric hydrogenation of MAA. The lower H_2 pressure of 2.3 MPa resulted in the lower MHB

yield, TOF_{30} value, and ee value, which was related to the lower solubility of H_2 in methanol at the lower pressure. When the H_2 pressure was increased to 4.6 MPa, a quantitative yield of MHB and a maximum TOF_{30} value of 800 h^{-1} were achieved. However, the further increase in H_2 pressure resulted in a rapid decrease in the TOF_{30} value. This decrease can be attributed to the accelerated solubility of H_2 in methanol as the hydrogen pressure rose, resulting in a reduction in the concentration of MAA surrounding Ru-**3a**. In addition, H_2 pressure had a little effect on ee values, and pressures above 4.6 MPa resulted in a slight decrease in ee values, most likely due to the diminished chiral induction of the chiral catalysts at higher pressures.[25,26] Therefore, a H_2 pressure of 4.6 MPa seemed optimal for the subsequent investigation.

The introduction of HBr in the preparation of [(**3a**)RuBr₂] catalyst provided two equivalents of Br^- as ligands for complexation with Ru(II). Some studies revealed that an excess of inorganic or organic acids could protonate the carbonyl group of the β-keto esters, facilitating hydride insertion in catalytic cycle, thus increasing overall catalytic activity.[27] The effect of HBr concentration on the Ru-**3a**-catalyzed asymmetric hydrogenation of MAA was depicted in Fig. 2C. When the molar ratio of HBr to Ru was 2.4 : 1, the yield of MHB was only 52% with low TOF_{30} and ee values, indicating that [(**3a**)RuBr₂] could not be formed effectively at the lower HBr concentrations. As the molar ratio of HBr to Ru was increased to 3.4 : 1, the highest yield, TOF_{30}, and ee values were observed. The continuous increase of HBr dosage led to the decrease of TOF_{30} and ee values, because the electrostatic repulsion of HBr as an electrolyte may promote the conversion of the active monomer [(**3**)RuBr₂] to the inactive dimer [(**3**)RuBr₂]₂, thus reducing the catalytic activity.[15] Therefore, the molar of HBr to Ru at 3.4 : 1 is optimal for achieving the desired catalytic performance.

3.4 Catalyst recyclability

In general, the classical homogeneous chiral Ru-BINAP catalysts cannot be effectively recovered without adding a carrier IL. CPF-PILs integrate the dual functions of phosphine ligand and IL, and can realize self-supporting and recycling without the need for an additional carrier IL, thus avoiding the negative effects of using larger quantities of carrier ILs. Based on to this feature of
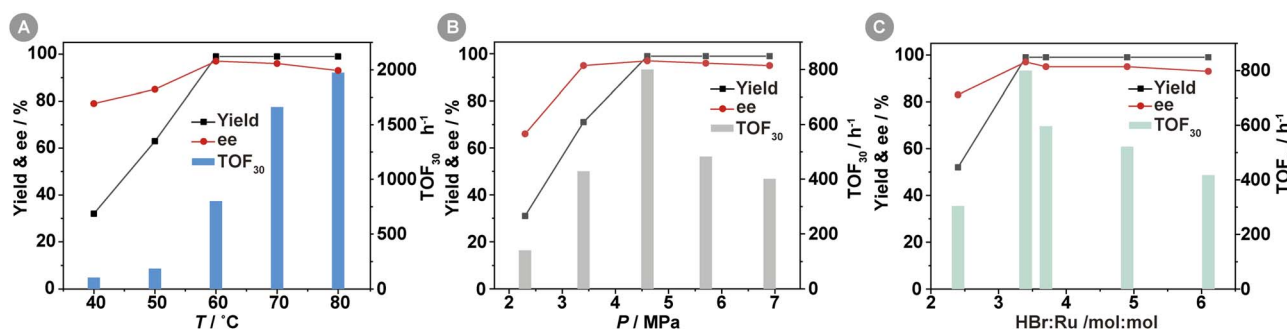

Fig. 2 Effect of reaction conditions on Ru-**3a**-catalyzed asymmetric hydrogenation of MAA. (A) Temperature, (B) H_2 pressure, (C) amount of HBr. Reaction conditions: Ru[(2-methylallyl)₂(COD)]: 1 mg, catalyst loading 0.1 mol%, $n(Ru) : n(\mathbf{3a}) : n(HBr) : n(MAA) = 1 : 1.2 : 3.4 : 1000$, 2 mL MeOH as solvent, $T = 60$ °C, $P(H_2) = 4.6$ MPa, $t = 3$ h.

CPF-PILs, we developed a homogeneous catalysis-biphasic separation (HCBS) system for the recovery and cycling of homogeneous chiral catalysts.[14,15] Fig. 3 depicted the model diagram of the HCBS system. In this system, the Ru-**3a** catalyst participates in a homogeneous catalytic hydrogenation within a methanol medium (a and b, Fig. 3). Following the reaction, the methanol is removed by vacuum, and the product is extracted using *n*-hexane, in which the product is soluble, but the catalyst is insoluble. The catalyst is precipitated and solidified in ice water to achieve a biphasic separation of the product and catalyst (c, Fig. 3).

Using asymmetric hydrogenation of MAA as the reaction model, the cycling stability of Ru-**3a** catalyst was investigated. As shown in Fig. 4, the TOF_{30} values indicated a rapid decreasing trend during the first five cycles, but MHB maintained the quantitative yields, and the ee values revealed a mild decrease, remaining at 87% after five runs. We infer that the reduction in TOF_{30} values may be due to the oxidation or loss of Ru-**3a**. However, ICP-AES analysis showed that Ru and P lost to the *n*-hexane-extraction phase was only 0.3–0.4% and 0.5–0.7%, respectively, indicating that the decreases in catalytic activity and enantioselectivity were not related to the loss of catalyst, but may be caused by the inevitable oxidation of phosphine ligand during the cycling process. To substantiate this claim, 0.6 equivalents of fresh **3a** were introduced into the system during the sixth cycle, restoring both TOF_{30} and ee values to their initial levels. This process was repeated during the 11th cycle, yielding a replication of the previously mentioned trend, proving that the decreased activity and ee values were indeed caused by the partial oxidation of **3a**. The ^{31}P NMR analysis performed on both fresh Ru-**3a** and Ru-**3a** that was run for 12 times fruther confirmed the oxidation of phosphine ligand. As depicted in the ^{31}P NMR spectrum of freshly prepared Ru-**3a** (a, Fig. 5), the resonance peaks of $[(\mathbf{3a})RuBr_2]$ and $[(\mathbf{3a})RuBr_2]_2$ were observed at δ 26.7 ppm and 27.3 ppm as well as the signals of residual free **3a** (δ −17.1 ppm) and phosphine monoxide of **3a** (δ −16.1 ppm) appeared in the high field.[15,28] In contrast, in the ^{31}P NMR spectrum of Ru-**3a** after 12 cycles (b, Fig. 5), the signal intensity of $[(\mathbf{3a})RuBr_2]$ as well as $[(\mathbf{3a})RuBr_2]_2$ decreased, and a distinct resonance peak of **3a**-dioxide at δ 30.6 ppm was observed.[29] In addition, we conducted an air stability experiment on Ru-**3a** in a nitrogen atmosphere containing 0.5%
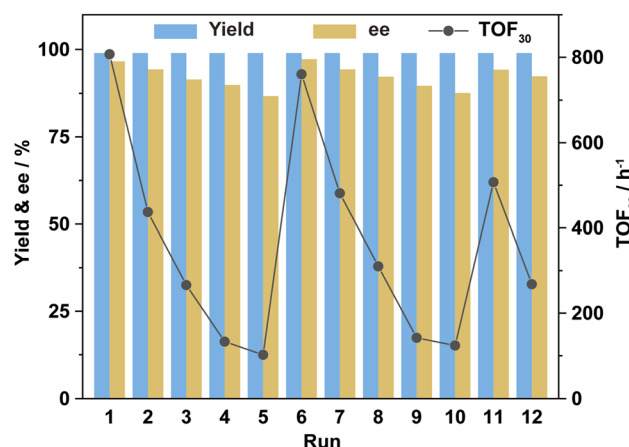

Fig. 4 Cycling experiments on Ru-**3a**-catalyzed asymmetric hydrogenation of MAA. Reaction conditions: Ru[(2-methylallyl)$_2$(COD)]: 1 mg, catalyst loading 0.1 mol%, n(Ru) : n(**3a**) : n(HBr) : n(MAA) = 1 : 1.2 : 3.4 : 1000, 2 mL MeOH, T = 60 °C, P(H$_2$) = 4.6 MPa, t = 20 h.

oxygen at 60 °C with stirring for 20 h. The ^{31}P NMR spectrum clearly showed the emergence of phosphine dioxide at 28.7 ppm (Fig. S1†), which further confirmed that the oxidation of the ligand during the cycling is the primary reason for the decline in catalytic efficiency. Also, to exclude the influence of the reaction temperature and moisture on Ru-**3a** catalyst, the thermal stability and moisture stability of Ru-**3a** were characterized by TG (Fig. S2†) and ^{31}P NMR spectroscopy (Fig. S3†), respectively, indicating that Ru-**3a** has high thermal stability and tolerance to moisture.

Ru-**3a** had a total turnover number (TTON) of 12 101 after 12 consecutive cycles, demonstrating the excellent recovery and cycling performances under the HCBS system. Although the oxidation of phosphine ligand causes a temporary decrease in TOF_{30} and ee values, the catalytic performance can be maintained at a high level for extended periods by intermittently supplementing with a few fresh phosphine ligands.

The catalytic performances of the CPF-PILs reported in this study was compared to that of catalysts previously reported in the literature for asymmetric hydrogenation of β-keto esters, as shown in Table S1.† In both IL-homogeneous and IL-biphasic catalytic systems (entries 1–12, Table S1†), the additional carrier ILs were required for supporting the chiral catalyst,
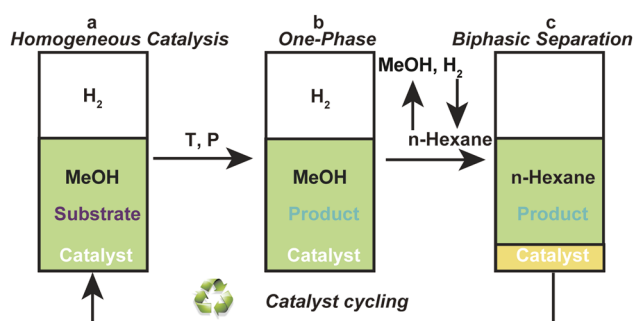

Fig. 3 The model diagram of the homogeneous catalysis-biphasic separation system: (a) homogeneous catalysis, (b) one-phase and (c) biphasic separation.
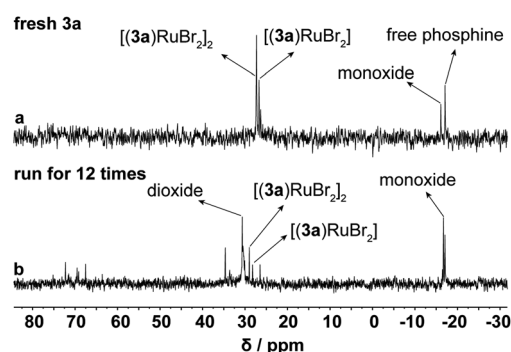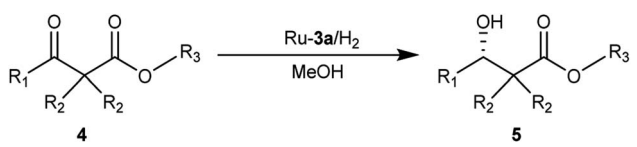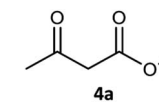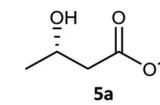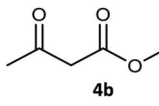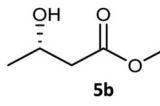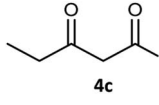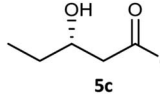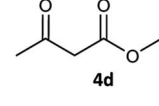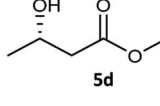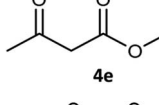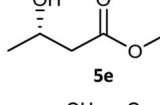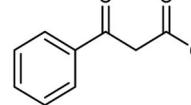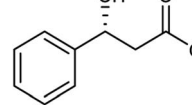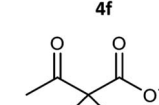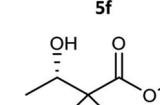

Fig. 5 ^{31}P NMR spectra of (a) freshly prepared and (b) recovered Ru-**3a** (202 MHz, DMSO-d_6).

Table 3 Asymmetric hydrogenation of structurally diverse β-keto esters catalyzed by Ru-**3a**[a]

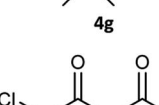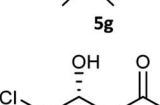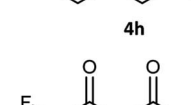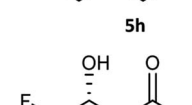| Entry	Substrate	Product	Yield[b]/%	ee (S or R)[b]/%	TOF$_{30}$/h^{-1}
1[c]	4a	5a	99	97 (S)	800
2	4b	5b	99	97 (S)	593
3	4c	5c	99	>99 (S)	469
4	4d	5d	99	96 (S)	396
5	4e	5e	99	93 (S)	176
6	4f	5f	99	96 (R)	103
7	4g	5g	99	99 (S)	368
8	4h	5h	99	99 (R)	320
9	4i	5i	65	10 (R)	41

[a] Reaction conditions: Ru[(2-methylallyl)$_2$(COD)]: 1 mg, catalyst loading 0.1 mol%, n(Ru):n(**3a**):n(HBr):n(β-keto ester) = 1:1.2:3.4:1000, 2 mL MeOH as solvent, P(H$_2$) = 4.6 MPa, T = 60 °C, t = 20 h. [b] Determined by GC using a Supelco γ-dex 225 (30 m × 0.25 mm × 0.25 μm) chiral capillary column. [c] t = 3 h.

being 20–3469 mol% of the substrate, and this enormous consumption is unacceptable. In contrast, the CPF-PILs with the self-supporting characteristics can achieve the efficient cycling of the chiral catalyst without the need for additional carrier ILs, which greatly reduces the negative effects of ILs on the catalytic reaction (entry 18, Table S1†). Although the supported ionic liquid phase (SILP) system in continuous gas phase hydrogenation can significantly reduce the amount of ILs (entry 13, Table S1†), the complex reactor design and operation impose limitations on their application.[30] The aqueous biphasic system is undoubtedly environmentally friendly, but the use of a large amount of water may lead to the decomposition of chiral catalysts (entries 14–16, Table S1†).[16,23,31,32] The thermoregulated catalytic system faces the issue of the complex synthesis process of ligands (entry 17, Table S1†).[33] In summary, the HCBS system in this study achieved the efficient asymmetric hydrogenation

of β-keto esters by using catalytic amounts of CPF-PILs, exhibiting superior or comparable catalytic performances to currently reported catalytic systems in terms of IL dosage, catalytic efficiency, enantioselectivity, service life and Ru loss.

3.5 General applicability

Table 3 examined the asymmetric hydrogenation of nine β-keto esters with different steric hindrance and electronic effects under optimized reaction conditions to investigate the generalizability of Ru-**3a** catalyst for the asymmetric hydrogenation of β-keto esters with different structures (Fig. S4†). Except for ethyl 4,4,4-trifluoroacetoacetate (**4i**) (entry 9, Table 3), all β-hydroxy esters were obtained in quantitative yields with high ee values of 93–99%, showing the excellent generalizability of Ru-**3a**. The TOF_{30} values were clearly dependent on steric hindrance as well as electron-donating and electron-withdrawing effects of R_1, R_2 and R_3 groups. TOF_{30} and ee values decreased significantly with the increase of the steric hindrance of the R_1, R_2 and R_3 groups due to the repulsion effect of the bulky group on the substrate to phenyl groups of the **3a**.[15,34,35] In addition, the incorporation of the electron-withdrawing substituent $-CH_2Cl$ (**4h**) or $-CF_3$ (**4i**) led to a reduction in the electron cloud density surrounding the carbonyl oxygen, which negatively impacted the interaction between the substrate and the Ru(II) center, consequently causing a significant decline in the TOF_{30} and/or ee values.[35,36] In particular, Ru-**3a** gave only 65% yield and 10% ee value when the R_1 was a strong electron-withdrawing group $-CF_3$ (entry 9, Table 3).

4 Conclusions

In conclusion, a new class of CPF-PILs was synthesized by an ion-exchange reaction between a phenyl-sulfonated BINAP chiral diphosphine ligand and polyether imidazolium ILs. The CPF-PILs were used in Ru-catalyzed homogeneous asymmetric hydrogenation of β-keto esters, and various β-keto esters were quantitatively converted to the corresponding β-hydroxy esters, yielding high ee values of 93–97%. Compared with the parent phenyl-sulfonated BINAP ligand, the CPF-PILs demonstrated a significant enhancement in the activity, which could be attributed to the spatial effect induced by the polyether group. Furthermore, the CPF-PILs showed superior catalytic performances in aprotic organic solvents, indicating the high tolerance for various organic solvents. Because of the dual function of CPF-PILs as both a chiral phosphine ligand and an IL, only a catalytic amount of CPF-PILs realized the efficient recovery and recycling of the chiral catalysts with no additional carrier ILs, allowing for environmentally friendly application of ILs. This study confirms that the concept of "integrated phosphine ligands and ILs" is universal for sulfonated chiral ligands, and provides a new solution for the green application of ILs in asymmetric hydrogenation.

Author contributions

Fan Wang: investigation, writing – review and editing, experimental scheme design, formal analysis. Shuai Zhang: experimental scheme design, formal analysis. Congxia Xie: formal analysis, validation. Xin Jin: conceptualization, experimental scheme design, writing – review and editing, funding acquisition.

Conflicts of interest

There are no conflicts to declare.

Acknowledgements

Notes and references

1 R. Noyori, Asymmetric catalysis: science and opportunities (Nobel lecture), *Angew. Chem., Int. Ed.*, 2002, **41**, 2008–2022.

2 P. Etayo and A. Vidal-Ferran, Rhodium-catalysed asymmetric hydrogenation as a valuable synthetic tool for the preparation of chiral drugs, *Chem. Soc. Rev.*, 2013, **42**, 728–754.

3 R. Noyori, *Asymmetric catalysis In organic synthesis*, Wiley, New York, 1994.

4 D. J. Cole-Hamilton, Homogeneous catalysis-new approaches to catalyst separation, recovery, and recycling, *Science*, 2003, **299**, 1702–1706.

5 P. Migowski, P. Lozano and J. Dupont, Imidazolium based ionic liquid-phase green catalytic reactions, *Green Chem.*, 2023, **25**, 1237–1260.

6 G. Kaur, H. Kumar and M. Singla, Diverse applications of ionic liquids: a comprehensive review, *J. Mol. Liq.*, 2022, **351**, 118556.

7 S. K. Singh and A. W. Savoy, Ionic liquids synthesis and applications: an overview, *J. Mol. Liq.*, 2020, **297**, 112038.

8 H. L. Ngo, A. Hu and W. Lin, Catalytic asymmetric hydrogenation of aromatic ketones in room temperature ionic liquids, *Tetrahedron Lett.*, 2005, **46**, 595–597.

9 M. Berthod, J. M. Joerger, G. Mignani, M. Vaultier and M. Lemaire, Enantioselective catalytic asymmetric hydrogenation of ethyl acetoacetate in room temperature ionic liquids, *Tetrahedron: Asymmetry*, 2004, **15**, 2219–2221.

10 X. Jin, J. Feng, Q. Ma, H. Song, Q. Liu, B. Xu, M. Zhang, S. Li and S. Yu, Integration of a phosphine ligand into an ionic liquid: a highly effective biphasic system for the Rh-catalyzed hydroformylation of 1-octene, *Green Chem.*, 2019, **21**, 3267–3275.

11 K. Huang, F. F. Chen, D. J. Tao and S. Dai, Ionic liquid-formulated hybrid solvents for CO_2 capture, *Curr. Opin. Green Sustainable Chem.*, 2017, **5**, 67–73.

12 X. Jin, S. Li and K. Zhao, CN Pat., CN201310370138.6, 2016.

13 X. Jin, F. Wang, L. Zhu and S. Li, CN Pat., CN202010385022.X, 2022.

14 X. Jin, J. Feng, H. Song, J. Yao, Q. Ma, M. Zhang, C. Yu, S. Li and S. Yu, Integration of phosphine ligands and ionic liquids both in structure and properties-a new strategy for

separation, recovery, and recycling of homogeneous catalyst, *Green Chem.*, 2019, **21**, 3583–3596.

15 F. Wang, S. Zhang, S. Huang, L. Zhu, H. Song, C. X. Xie and X. Jin, Integration of chiral phosphine ligand and ionic liquids: sustainable and functionally enhanced BINAP-based chiral Ru(II) catalysts for enantioselective hydrogenation of β-keto esters, *Green Chem.*, 2023, **25**, 6432–6445.

16 K. Wan and M. E. Davis, Asymmetric hydrogenation in water by a rhodium complex of sulfonated 2,2'-bis (diphenylphosphino)-1,1'-binaphthyl (binap), *Chem. Commun.*, 1993, **16**, 1262–1264.

17 H. S. Schrekker, D. O. Silva, M. A. Gelesky, M. P. Stracke, C. M. L. Schrekker, R. S. Gonçalves and J. Dupont, Preparation, cation-anion interactions and physicochemical properties of ether-functionalized imidazolium ionic liquids, *J. Braz. Chem. Soc.*, 2008, **19**, 426–433.

18 W. L. F. Armarego and C. L. L. Chai, *Purification of laboratory chemicals*, Elsevier/Butterworth-Heinemann, Burlington, MA, USA, 5th edn, 2003.

19 V. Ratovelomanana-Vidal, C. Girard, R. Touati, J. P. Tranchier, B. B. Hassine and J. P. Genêt, Enantioselective hydrogenation of β-keto esters using chiral diphosphine-ruthenium complexes: optimization for academic and industrial purposes and synthetic applications, *Adv. Synth. Catal.*, 2003, **345**, 261–274.

20 C. Reichardt and T. Welton, *Solvents and solvent effects in organic chemistry*, Weinheim, John Wiley & Sons, 4th edn, 2011.

21 C. Reichardt, Solvation effects in organic chemistry: a short historical overview, *J. Org. Chem.*, 2021, **87**, 1616–1629.

22 M. J. Kamlet, J. L. M. Abboud, M. H. Abraham and R. W. Taft, Linear solvation energy relationships. 23. A comprehensive collection of the solvatochromic parameters, π^*, α, and β, and some methods for simplifying the generalized solvatochromic equation, *J. Org. Chem.*, 1983, **48**, 2877–2887.

23 A. Wolfson, I. F. J. Vankelecom, S. Geresh and P. A. Jacobs, The role of the solvent in the asymmetric hydrogenation of β-keto esters with Ru-BINAP, *J. Mol. Catal. A: Chem.*, 2003, **198**, 39–45.

24 R. Noyori and T. Ohkuma, Asymmetric catalysis by architectural and functional molecular engineering: practical chemo-and stereoselective hydrogenation of ketones, *Angew. Chem., Int. Ed.*, 2001, **40**, 40–73.

25 A. Berger, R. F. de Souza, M. R. Delgado and J. Dupont, Ionic liquid-phase asymmetric catalytic hydrogenation: hydrogen concentration effects on enantioselectivity, *Tetrahedron: Asymmetry*, 2001, **12**, 1825–1828.

26 K. Wan and M. E. Davis, Ruthenium(II)-sulfonated BINAP: a novel water-soluble asymmetric hydrogenation catalyst, *Tetrahedron: Asymmetry*, 1993, **4**, 2461–2468.

27 A. Wolfson, I. F. J. Vankelecom, S. Geresh and P. A. Jacobs, The role of acid in accelerating the asymmetric reduction of methyl acetoacetate with BINAP-chloro-(*p*-cymene)-Ru chloride complex, *J. Mol. Catal. A: Chem.*, 2004, **217**, 21–26.

28 F. Ozawa, A. Kubo and T. Hayashi, Generation of tertiary phosphine-coordinated Pd(0) species from Pd(OAc)$_2$ in the catalytic Heck reaction, *Chem. Lett.*, 1992, **21**, 2177–2180.

29 H. Takaya, K. Mashima, K. Koyano, M. Yagi, H. Kumobayashi, T. Taketomi, S. Akutagawa and R. Noyori, Practical synthesis of (*R*)-or (*S*)-2,2'-bis (diarylphosphino)-1,1'-binaphthyls (BINAPs), *J. Org. Chem.*, 1986, **51**, 629–635.

30 E. Öchsnera, M. J. Schneidera, C. Meyera, M. Haumannb and P. Wasserscheid, Challenging the scope of continuous, gas-phase reactions with supported ionic liquid phase (SILP) catalysts—Asymmetric hydrogenation of methyl acetoacetate, *Appl. Catal., A*, 2011, **399**, 35–41.

31 X. Jin, S. Huang, F. Wang, L. Zhu, H. Song, C. Xie, S. Yu and S. Li, Synthesis and characterization of a high-purity chiral 5,5'-disulfonato-BINAP ligand and its application in asymmetric hydrogenation of β-keto esters, *Mol. Catal.*, 2021, **507**, 111562.

32 K. Mashima, K. Kusano, N. Sato, Y. Matsumura, K. Nozaki, H. Kumobayashi, N. Sayo, Y. Hori, T. Ishizaki, S. Akutagawa and H. Takaya, Cationic BINAP-Ru(II) halide complexes: highly efficient catalysts for stereoselective asymmetric hydrogenation of. α-and. β-functionalized ketones, *J. Org. Chem.*, 1994, **59**, 3064–3076.

33 Y.-Y. Huang, Y.-M. He, H.-F. Zhou, L. Wu, B.-L. Li and Q.-H. Fan, Thermomorphic system with non-fluorous phase-tagged Ru (BINAP) catalyst: facile liquid/solid catalyst separation and application in asymmetric hydrogenation, *J. Org. Chem.*, 2006, **71**, 2874–2877.

34 S. Kong, A. U. Malik, X. Qian, M. Shu and W. Xiao, Asymmetric hydrogenation of β-keto esters catalyzed by ruthenium species supported on porous organic polymer, *Chinese J. Org. Chem.*, 2018, **38**, 656–664.

35 L. Chen, M.-L. Ma, Z.-H. Peng and H. Chen, Synthesis of a new bipyridyl diphosphine ligand and its application to asymmetric hydrogenation of β-keto esters, *Chinese J. Org. Chem.*, 2008, **28**, 1724–1728.

36 D. Blanc, V. Ratovelomanana-Vidal, J. P. Gillet and J. P. Genêt, Asymmetric synthesis of fluorinated β-hydroxy esters via ruthenium-mediated hydrogenation, *J. Organomet. Chem.*, 2000, **603**, 128–130.